Evidence for a Novel Quinone-Binding Site in the Photosystem II (PS II) Complex That Regulates the Redox Potential of Cytochrome b559

Olga Kaminskaya,[‡] Vladimir A. Shuvalov,[‡] and Gernot Renger*[,§]

Institute of Basic Biological Problems, Russian Academy of Sciences, Pushchino, Moscow Region 142290, Russia, and Max-Volmer-Laboratory, Technical University Berlin, Strasse des 17. Juni 135, 10623 Berlin, Germany

Received June 29, 2006; Revised Manuscript Received November 23, 2006

ABSTRACT: The present study provides a thorough analysis of effects on the redox properties of cytochrome (Cyt) b559 induced by two photosystem II (PS II) herbicides [3-(3,4-dichlorophenyl)-1,1-dimethylurea (DCMU) and 2,4-dinitro-6-*sec*-butylphenol (dinoseb)], an acceleration of the deactivation reactions of system Y (ADRY) agent carbonylcyanide-*m*-chlorophenylhydrazone (CCCP), and the lipophilic PS II electron-donor tetraphenylboron (TPB) in PS II membrane fragments from higher plants. The obtained results revealed that (1) all four compounds selectively affected the midpoint potential (E_m) of the high potential (HP) form of Cyt b559 without any measurable changes of the E_m values of the intermediate potential (IP) and low potential (LP) forms; (2) the control values from +390 to +400 mV for HP Cyt b559 gradually decreased with increasing concentrations of DCMU, dinoseb, CCCP, and TPB; (3) in the presence of high TPB concentrations, a saturation of the E_m decrease was obtained at a level of about +240 mV, whereas no saturation was observed for the other compounds at the highest concentrations used in this study; (4) the effect of the phenolic herbicide dinoseb on the E_m is independent of the occupancy of the Q_B-binding site by DCMU; (5) at high concentrations of TPB or dinoseb, an additional slow and irreversible transformation of HP Cyt b559 into IP Cyt b559 or a mixture of the IP and LP Cyt b559 is observed; and (6) the compounds stimulate autoxidation of HP Cyt b559 under aerobic conditions. These findings lead to the conclusion that a binding site Q_C exists for the studied substances that is close to Cyt b559 and different from the Q_B site. On the basis of the results of the present study and former experiments on the effect of PQ extraction and reconstitution on HP Cyt b559 [Cox, R. P., and Bendall, D. S. (1974) The functions of plastoquinone and β-carotene in photosystem II of chloroplasts, *Biochim. Biophys. Acta 347*, 49−59], it is postulated that the binding of a plastoquinone (PQ) molecule to Q_C is crucial for establishing the HP form of Cyt b559. On the other hand, the binding of plastoquinol (PQH_2) to Q_C is assumed to cause a marked decrease of E_m, thus, giving rise to a PQH_2 oxidase function of Cyt b559. The possible physiological role of the Q_C site as a regulator of the reactivity of Cyt b559 is discussed.

The multimeric complex of photosystem II (PS II)[1] of all oxygen-evolving photosynthetic organisms acts as a light-driven water−plastoquinone (PQ) oxidoreductase, where the cofactors involved in this function are bound to a heterodimeric protein matrix consisting of polypeptides D1 and D2 (see refs *1*−*3* as general reviews). Light-induced charge separation leads to the formation of the "stable" radical pair, $P680^{+\cdot}Q_A^{-\cdot}$ (*4*), followed by two reaction sequences: (i) PQ reduction to quinol with $Q_A^{-\cdot}$ as a reductant and (ii) oxidative water cleavage into molecular oxygen and four protons, with $P680^{+\cdot}$ providing the driving forces. The plastoquinol (PQH_2) formation process takes place at the Q_B site, where the noncovalently bound PQ-molecule Q_B is reduced by $Q_A^{-\cdot}$ via a sequence of two one-electron steps, concomitant with H^+ uptake (*5*). This process closely resembles that of quinol formation in the reaction center of anoxygenic photosynthetic bacteria (*4*). The Q_B-binding niche is also the binding site for PS II herbicides that replace the native quinone Q_B, thus, leading to a blockage of $Q_A^{-\cdot}$ reoxidation by Q_B ($Q_B^{-\cdot}$) (see refs *6*−*12* for reviews). In marked contrast to charge separation and quinol formation, which are similar in anoxygenic purple bacteria and oxygenic photosynthesis (*4*, *8*), the oxidative water cleavage is unique for oxygen-evolving organisms. This process takes place at a manganese-containing catalytic site of the water-oxidizing complex (WOC) and comprises a sequence of four redox steps (reviewed in refs *2*, *13*, and *14*).

Apart from the presence of the WOC, there exists another striking difference between purple bacteria reaction centers and PS II of oxygenic photosynthesis. The PS II complex

* To whom correspondence should be addressed. Telephone: +49-30-314-22-794. Fax: +49-30-314-21-122. E-mail: rengsbbc@mailbox.tu-berlin.de.

‡ Russian Academy of Sciences.

§ Technical University Berlin.

[1] Abbreviations: PS II, photosystem II; Cyt, cytochrome; WOC, water-oxidizing complex; Chl, chlorophyll; Car, carotenoid; E_m, midpoint potential; HP, high potential; IP, intermediate potential; LP, low potential; IM, intermediate; TPB, tetraphenylboron; ADRY, acceleration of the deactivation reactions of system Y; CCCP, carbonylcyanide-*m*-chlorophenylhydrazone; FCCP, carbonylcyanide-*p*-trifluoromethoxyphenylhydrazone; ANT2p, 2-(3-chloro-4-trifluoromethyl)-aniline-3,5-dinitrothiophene; DCMU, 3-(3,4-dichlorophenyl)-1,1-dimethylurea; dinoseb, 2,4-dinitro-6-*sec*-butylphenol; MES, 2-[*N*-morpholino]ethanesulfonic acid; HOQNO, 2-*n*-heptyl 4-hydroxyquinoline-*N*-oxide; PQ, plastoquinone; PQH_2, plastoquinol.

10.1021/bi0613022 CCC: $37.00
Published on Web 12/30/2006

of both higher plants and cyanobacteria contains the tightly bound integral heme protein cytochrome (Cyt) b559 (see refs *15*−*17* for reviews). X-ray structural analyses with resolutions of 3.8−3.0 Å of crystals from PS II complexes of the two thermophilic cyanobacteria *Thermosynechococcus elongatus* and *Thermosynechococcus vulcanus* (*18*−*23*) reveal that the two subunits PsbE and PsbF of Cyt b559 are located near the D2 protein. The heme iron is coordinated by two axial histidine ligands of both subunits (PsbE and PsbF), each containing a single His and forming one transmembrane helix (*24*−*30*). The heme group of Cyt b559 is located near the cytosolic surface (*27*, *30*) at a center−center distance of about 30 Å to Q_B (*23*) and is characterized by unique redox properties.

In PS II membrane fragments from higher plants, Cyt b559 exists in three forms characterized by a different midpoint potential (E_m) of the heme group (*31*−*37*). At pH 6.5, the dominant form exhibits an unusually high midpoint potential with an E_m value from +390 to +400 mV [high potential (HP) form] and a relative population of typically 70%. The remaining minor fractions are present in varying amounts of the intermediate potential (IP) form with an E_m from +200 to +250 mV and the low potential (LP) form with an E_m from +50 to +100 mV.

The functional role of Cyt b559 in PS II is still not yet completely clarified. Several possibilities have been discussed (*15*−*17*). A common view considers Cyt b559 as a member of the cyclic electron pathway, which contributes to the protection of PS II against photoinhibition. In this reaction, oxidized Cyt b559 is assumed to operate as an electron acceptor for either the reduced PQH_2 pool, the bound semiquinone $Q_B^{-\cdot}$, or Q_BH_2 (*38*−*42*) and the reduced heme group acts as an electron donor to $P680^{+\cdot}$, with carotenoid (Car) and, presumably, chlorophyll $(Chl)_Z$ as intermediate redox active group(s). Recently, Cyt b559 has been proposed to function as a catalyst for the oxidation of the reduced PQ pool by molecular oxygen (*43*−*45*).

The origin of the differences between the HP, IP, and LP redox forms of Cyt b559 is not yet resolved. Several possibilities have been considered: (i) variation in the mutual orientation of the planes of the axial histidine ligands of the heme group (*26*), (ii) modifications of the protonation and/or hydrogen-bonding pattern of axial ligands (*31*, *37*, *46*−*48*), (iii) changes in the polarity of the dielectric environment of the heme (*49*), or (iv) changes in the nature of heme coordination (*36*).

The configuration related to the structure of HP Cyt b559 is unstable toward different treatments including aging, heat and high pH treatments, and increased concentrations of salts and detergents (*15*, *31*, *32*, *34*, *36*, *50*−*55*). As the result of such treatments, HP Cyt b559 is transformed into the IP form or a mixture of the IP and LP forms.

A transformation of HP Cyt b559 to lower potential form(s) is suggested to be induced also by the so-called acceleration of the deactivation reactions of system Y (ADRY) reagents, such as carbonylcyanide-*p*-trifluoromethoxyphenylhydrazone (FCCP), carbonylcyanide-*m*-chlorophenylhydrazone (CCCP), and 2-(3-chloro-4-trifluoromethyl)aniline-3,5-dinitrothiophene (ANT2p) (*31*, *56*). These highly lipophilic aromatic compounds, which contain a moderately acidic NH (or OH) group, catalyze a pathway for the fast reduction of the redox states S_2 and S_3 of the WOC (*57*−*60*). A very efficient electron donation to WOC was also found for the lipophilic tetraphenylboron (TPB) anion (*61*−*63*), but unlike "true" ADRY compounds, TPB is irreversibly consumed in this reacton (*62*, *63*). The interactions of ADRY-type reagents and TPB with Cyt b559 cause its oxidation in the dark and, to a larger extent, under illumination (*15*, *31*, *41*, *56*, *64*−*70*). These effects have been assigned to the transformation of HP Cyt b559 to an autoxidizible LP form. Transformation of HP Cyt b559 into the LP form was also reported to be induced by the PS II herbicide 2,4-dinitro-6-*sec*-butylphenol (dinoseb) at millimolar concentrations (*71*).

The underlying mechanism(s) of these effects are not yet clarified. Therefore, the present study was performed to address this point. Thorough analyses of effects induced by PS II herbicides [3-(3,4-dichlorophenyl)-1,1-dimethylurea (DCMU) and dinoseb], the lipophilic anion TPB, and a typical ADRY compound CCCP were performed on the basis of measurements of the redox pattern of Cyt b559. The results obtained reveal that all studied compounds specifically interact with HP Cyt b559 and provide evidence for the existence of an additional binding site for them within the PS II complex, which is different from the well-characterized Q_B site. The implications of these findings are discussed.

MATERIALS AND METHODS

PS II membrane fragments from sugar beet were isolated according to the procedure in ref *72* with some modifications (*73*). All assays were performed in buffer medium containing 100 mM 2-[*N*-morpholino]ethanesulfonic acid (MES) (pH 6.5), 0.4 M sucrose, 15 mM NaCl, 10 mM $CaCl_2$, and 10% glycerol at 20 °C. DCMU, dinoseb, and CCCP were dissolved in ethanol. The maximal amount of ethanol in samples containing high concentrations of herbicides was 1.6%. After the addition of DCMU, dinoseb, TPB, or CCCP, the samples were incubated anaerobically for 15 min before the beginning of the redox titration if another procedure is not specially indicated.

Difference absorbance spectra of Cyt b559 were recorded in the spectrophotometer Cary 4000 with an optical slit width of 2.5 nm in the range of 520−590 nm as previously described (*55*). The amplitude of absorbance changes at 560 nm in the difference spectra of Cyt b559 was determined relative to a line connecting reference points at 546 and 573 nm. The total amount of Cyt b559 was determined by measuring difference spectra of "dithionite-reduced minus $K_3[Fe(CN)_6]$-oxidized" Cyt b559. The amount of initially reduced Cyt b559 was gathered from the amplitude of its chemical oxidation by the addition of 100 μM $K_3[Fe(CN)_6]$. The Chl concentration was determined according to ref *74*. In all assays, it was in the range of 30−60 μg/mL.

Anaerobic redox titration of Cyt b559 was performed by measuring difference absorbance spectra at various ambient redox potentials of the suspension as previously described (*36*, *55*). Anaerobic conditions were achieved by a constant flow of argon above the sample solution and by the addition of 0.25 mg/mL glucose oxidase, 0.05 mg/mL catalase, and 5 mM glucose to the assay medium. $K_3[Fe(CN)_6]$ and freshly prepared sodium dithionite were used as the oxidant and reductant, respectively, and the following redox mediators were added: 1,4-benzoquinone, 2,3,5,6-tetramethyl-*p*-phe-

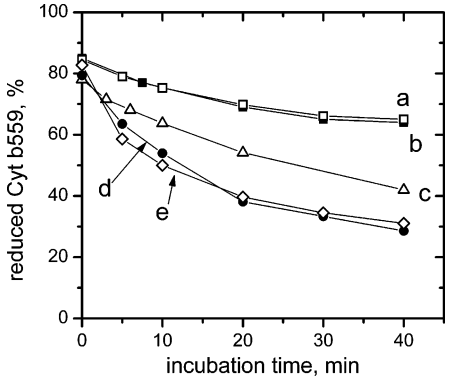

FIGURE 1: Dark oxidation of Cyt b559 in suspensions of PS II membrane fragments. The percentage of reduced Cyt b559 was determined at different time intervals after the suspension of concentrated samples of PS II membranes in the assay medium containing either no further additions (a), 20 μM DCMU (b), 25 μM dinoseb (c), 320 μM DCMU (d), or 1 μM TPB (e).

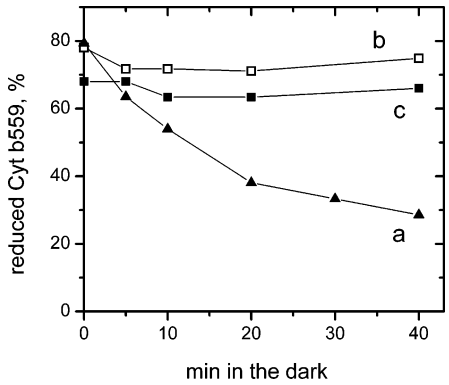

FIGURE 2: Relative amplitude of reduced Cyt b559 as a function of the incubation time in suspensions of PS II membrane fragments incubated in the dark in the presence of 320 μM DCMU under different redox conditions. Concentrated samples of PS II membranes were suspended in the assay medium in the presence of 320 μM DCMU containing either no further additions (a), supplemented with the system glucose/glucose oxidase to maintain anaerobiosis (b), or redox-buffered at +300 mV under aerobic conditions (c). In sample c, 100 μM $K_3[Fe(CN)_6]$ was added together with approximately 16 mM $K_4[Fe(CN)_6]$ in the assay medium to adjust the ambient redox potential to +300 mV. For further details, see the Materials and Methods.

nylenediamine, 2,5-dimethyl-1,4-benzoquinone, $FeSO_4$−ethylenediaminetetraacetic acid (EDTA) complex, 2-methyl-1,4-naphtoquinone at concentrations of 50 μM; 2-hydroxy-1,4-naphtoquinone at a concentration of 20 μM; *N*-methylphenazonium methosulfate and *N*-methylphenazonium ethosulfate at concentrations of 10 μM.

Both reductive and oxidative redox titrations were performed in each experiment, mostly using one and the same sample. Each point in Figures 4, 5, 7, 8, 10, and 11 represents the average of the values obtained in the two titration experiments of opposite direction. The difference between the midpoint potentials of HP Cyt b559 gathered from oxidative and reductive titrations was normally within 8−10 mV. Potentiometric Nernst curves were analyzed by a nonlinear curve-fitting Origin program.

Furthermore, we carefully checked for possible effects caused by the solvent addition from the stock solutions of the added compounds. The results obtained at the maximal ethanol content of 1.6% were virtually the same as those of the control without the addition of this solvent (for the sake of clarity, the data points are not explicitly shown in the figures, but data evaluation clearly illustrates the findings; see caption of Figure 4).

RESULTS

Untreated samples of PS II membrane fragments from sugar beet used in this study contained 70−80% of total Cyt b559 in the reduced state. This fraction reflects the content of initially reduced HP and IP forms of Cyt b559 (*36*). Figure 1 demonstrates effects of the slow partial oxidation of HP Cyt in suspensions of PS II membrane fragments incubated in the dark at 20 °C under aerobic conditions.

Curve a in Figure 1 shows that in untreated samples the initially reduced Cyt b559 is very slowly oxidized in the dark, reaching a level of 66% after 40 min of sample incubation. This small effect may reflect an autoxidation of initially reduced IP Cyt b559. Figure 1 further shows that the extent of slow dark oxidation of Cyt b559 is unaffected by the addition of 20 μM DCMU (curve b) but is significantly enhanced in samples that contained higher amounts of DCMU (curve d), another PS II herbicide, dinoseb (curve c), or the lipophilic anion TPB (curve e). A comparison of curves b and d of Figure 1 reveals that the DCMU concentrations, which are required for stimulation of the dark oxidation of Cyt b559, cover a range of hundreds of micromolars, i.e., are much higher than necessary for the blockage of Q_A^- reoxidation by Q_B (*75*−*79*). Further studies were performed to elucidate underlying mechanisms of effects on the redox state of Cyt b559 induced by TPB, DCMU, and dinoseb.

Figure 2 demonstrates that the dark oxidation of HP Cyt b559 caused by the presence of 320 μM DCMU (curve a) is completely eliminated either by anaerobiosis (curve b) or by the buffering of the redox potential of the medium at 300 mV under aerobic conditions (curve c). These findings show that (i) atmospheric oxygen acts as an electron acceptor in the process of HP Cyt b559 dark oxidation and (ii) slow autoxidation of HP Cyt b559 is not the result of a transformation of the HP form into lower redox potential forms (IP or LP). The latter conclusion is confirmed by a crucial check experiment, where $K_4[Fe(CN)_6]$ added at millimolar concentrations to samples containing Cyt b559 autooxidized in the presence of 320 μM DCMU restores the initial level of reduced Cyt b559 (data not shown). Therefore, the underlying mechanism of the DCMU effect described above is principally different from that earlier suggested for ADRY agents (*31*, *56*).

The latter conclusion was additionally checked by performing redox titrations of Cyt b559 in PS II membrane fragments after 40 min of dark oxidation of Cyt b559 in the presence of 320 μM DCMU. The results obtained are shown in Figure 3.

Data fitting and a comparison with the untreated control sample (curve a) reveal that neither the midpoint potentials of the three redox forms nor their relative contributions were significantly effected by a long incubation with 320 μM DCMU (curve b). The only discernible effect observed is a slight down shift of the E_m of HP Cyt b559 from +395 to +365 mV. It is important to note that in all redox titrations

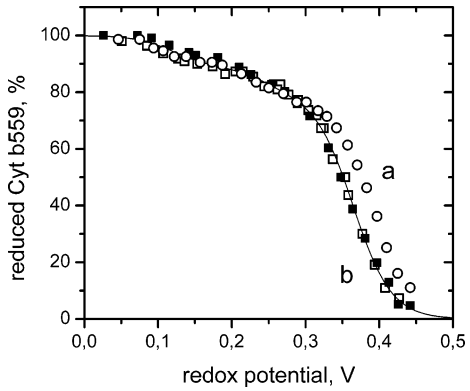

FIGURE 3: Relative amplitude of reduced Cyt b559 as a function of the redox potential in suspensions of untreated PS II membrane fragments in the absence (a) and presence (b) of 320 μM DCMU. Redox titration of Cyt b559 in sample b was performed in the presence of 320 μM DCMU after preincubation of an aerobic sample for 40 min in the presence of 320 μM DCMU. Open and closed symbols represent the data obtained in oxidative and reductive redox titrations, respectively. The best fit of the data points of sample a is a sum of three one-electron components with E_m values of +395, +247, and +116 mV with relative amplitudes of 75, 16, and 9%, respectively (the fitting curve and the data for reductive titration are not shown for the sake of simplicity; see refs *36* and *55* for details). It must be emphasized that, despite the comparatively small amplitudes, the IP and LP forms are clearly distinguished components as outlined in refs *36* and *55*. Furthermore, we have also carefully checked for a possible contribution of other components, e.g., originating from Cyt b_6f. As outlined in detail in our previous studies (*36*, *55*), the spectral analyses confirmed that the data reflect only Cyt b559. The best fit for the data points of sample b is a sum of three one-electron components with E_m values of +365, +246, and +120 mV and relative amplitudes of 79, 10, and 11%, respectively.

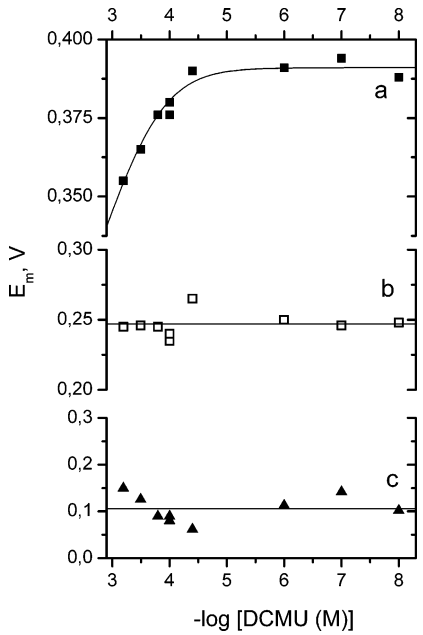

FIGURE 4: Midpoint potentials of HP (a), IP (b), and LP (c) redox forms of Cyt b559 as functions of the DCMU concentration in suspensions of PS II membrane fragments. Redox titrations of Cyt b559 were performed in suspensions of PS II membrane fragments containing different amounts of DCMU. The scalings of the ordinate for the HP, IP, and LP Cyt b559 are different as shown. Each point in the figure represents the average of the two titration experiments; the maximal difference between the E_m values in repetitive experiments did not exceed 10 mV. The full-line curve for the data set (a) represents the best fit by eq 1 (see the Discussion) with the following parameters: $pK_{ox}^{DCMU} = 3.7$, maximal $pK_{red}^{DCMU} = 2.0$, and $E_m([DCMU] = 0) = +391$ mV. The redox pattern of Cyt b559 in a control sample without DCMU containing the maximal amount of ethanol used in this study (1.6%) was best-fitted by three one-electron components with E_m values of +386, +228, and +109 mV and relative amplitudes of 73, 15, and 12%, respectively.

performed in the present study both oxidative and reductive titrations were carried out in one and the same sample, unless indicated otherwise. These titrations in opposite directions were usually separated by a time interval of 50−60 min. The data points in curve b of Figure 3 show that both titration curves (in oxidative and reductive directions) are virtually identical. This finding further demonstrates that no irreversible changes in the properties of the heme group (stable HP to IP/LP transformation) take place during an even longer incubation at high (320 μM) DCMU concentrations.

To unravel the origin of the small effect on the E_m value of HP Cyt b559 induced by 320 μM DCMU, the redox pattern of Cyt b559 was studied as a function of the DCMU concentration. The results obtained (depicted in Figure 4 in a logarithmic scale of the DCMU concentration) clearly show that in accordance with the data of Figure 3 only the HP form is affected by DCMU.

The midpoint potential of HP Cyt b559 gradually decreases with increasing DCMU concentrations. At the highest DCMU concentration of 640 μM, the E_m value shifts down to +355 mV. It must be emphasized that the results of oxidative and reductive titrations at different concentrations of DCMU in the same sample again showed the absence of any irreversible time-dependent modifications of the redox properties of the heme group during the course of the titration experiments. In marked contrast to the response of HP Cyt b559 (Figure 4a), the other forms (IP and LP) do not exhibit an analogous dependence of E_m on the DCMU concentration (parts b and c of Figure 4). The much higher scattering of these data compared with those of HP Cyt b559 is explained by the significantly lower relative amplitudes of the IP and LP components in the redox titration curves.

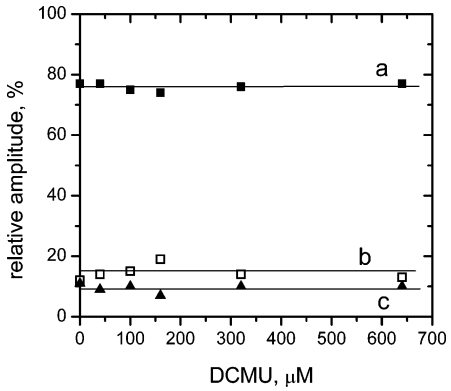

FIGURE 5: Relative amplitudes of HP (a), IP (b), and LP (c) forms of Cyt b559 in PS II membrane fragments as functions of the DCMU concentration. The relative amplitudes of the HP, IP, and LP Cyt b559 were gathered from titration experiments performed in samples containing different amounts of DCMU.

Figure 5 shows the dependence on the DCMU concentration of the relative amplitudes of the three forms of Cyt b559 (HP, IP, and LP) derived from the redox titration curves. These data provide clear evidence for the invariance of the

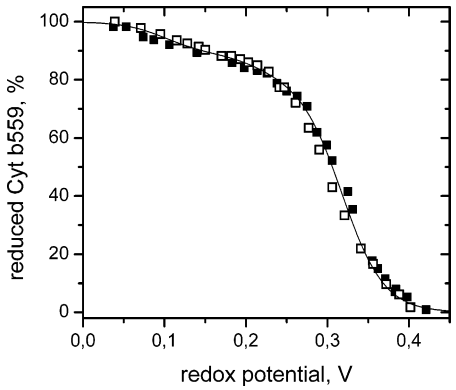

FIGURE 6: Relative amplitude of reduced Cyt b559 as a function of the redox potential in a suspension of PS II membrane fragments containing 110 μM dinoseb. Closed and open symbols represent the data points for reductive and oxidative titrations, respectively. The full line is the best fit with a sum of the three one-electron components with E_m values of +318, +217, and +101 mV and relative amplitudes of 81, 8, and 11%, respectively.

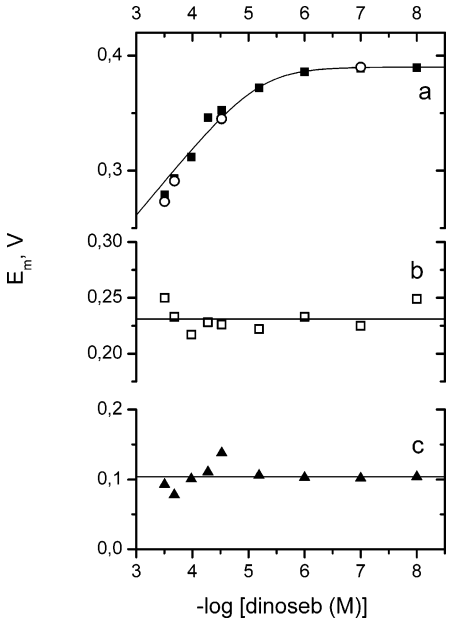

FIGURE 7: Midpoint potentials of the HP (a), IP (b), and LP (c) redox forms of Cyt b559 as functions of the dinoseb concentration in suspensions of PS II membrane fragments. Redox titrations of Cyt b559 were performed on PS II membrane fragments suspended either in the presence (○) or absence (■, □, and ▲) of 40 μM DCMU at different amounts of dinoseb. The scalings of the ordinate for the E_m values of the three redox forms of Cyt b559 are different as shown. The full-line curve for the data set (a) represents the best fit by eq 1 (see the Discussion) with the following parameters: $pK_{ox}^{dino} = 5.18$, maximal $pK_{red}^{dino} = 1.8$, and $E_m([dinoseb] = 0) = +390$ mV. For further details, see the Materials and Methods.

fractions of HP, IP, and LP forms of Cyt b559 within the whole range of DCMU concentrations.

The data of Figure 1 demonstrate also that the phenolic-type PS II herbicide dinoseb stimulates an oxidation of Cyt b559 in the dark. Because the mode of action on PS II differs between DCMU and dinoseb (see the Discussion), we analyzed the effect of dinoseb on the redox properties of Cyt b559 in more detail. Figure 6 shows the oxidative and reductive titration curves of Cyt b559 in PS II membrane fragments in the presence of 110 μM dinoseb. The data fit reveals that, in analogy to the action of DCMU, exclusively, the E_m of the HP form is affected among the three forms of Cyt b559. A decrease of the E_m value down to +318 mV at 110 μM dinoseb is observed.

Figure 7 presents a plot of E_m values of the HP, IP, and LP forms of Cyt b559 as a function of the negative logarithm of the dinoseb concentration (*p*[dinoseb]). These results show that, qualitatively, the same pattern is observed as that for DCMU; i.e., the HP form of Cyt b559 exhibits a decrease in the E_m with increasing concentrations of dinoseb.

In marked contrast to DCMU, where the onset of the E_m decrease (Figure 4a) and the inhibition of the linear electron transport in PS II (*75*, *78*, *79*) occur at quite different concentrations, in the case of dinoseb, both effects emerge in the same concentration range. Indeed, K_i values of 1−3 μM are reported for PS II inhibition by dinoseb (*79*−*81*), which cover the same range of the concentrations where the onset of the E_m decrease in Figure 7 arises. Therefore, it might be possible that the dinoseb effect on the E_m of HP Cyt b559 is related to the binding of this phenolic herbicide to the Q_B site.

To check for the latter possibility, redox titration experiments were performed in the presence of both dinoseb and 40 μM DCMU. This DCMU concentration is high enough to fully saturate the binding to the Q_B site, but on the other hand, it is sufficiently low to induce only a negligible effect on the E_m of HP Cyt b559 (see Figure 4). The open circles in Figure 7 represent the E_m values of HP Cyt b559 obtained in the presence of different dinoseb concentrations and 40 μM DCMU. The data points obtained in the absence and presence of 40 μM DCMU are virtually identical. Furthermore, the addition of 40 μM DCMU to the titration medium that already contained different amounts of dinoseb neither changed the relative amplitudes of the HP, IP, and LP forms in the titration curves nor induced the appearance of a HP form with an E_m value close to +390 mV, which is characteristic for the E_m of HP Cyt b559 in the presence of 40 μM DCMU alone. These findings clearly demonstrate that the occupancy of the Q_B site by the DCMU molecule does not affect the interaction of dinoseb with HP Cyt b559. Accordingly, PS II herbicides are capable of binding to a site in PS II that is at or near HP Cyt b559 and is different from the Q_B site. In the following sections, this "new" binding site will be symbolized by Q_C.

Unlike the experiments with DCMU, in the case of dinoseb, we found that high concentrations of this phenolic herbicide induced a transformation of HP Cyt b559 to the IP form, and this effect is time-dependent. Figure 8 shows the relative contents of the three redox forms of Cyt b559, derived from the titration curves, as functions of the dinoseb concentration. The data of Figure 8A correspond to the titration experiments described by Figure 7 and are obtained when the redox titration is carried out after 15 min of incubation of the sample in the presence of dinoseb. The same conditions were used in the experiments with DCMU shown in Figures 4 and 5. In the case of dinoseb, the relative amounts of the three forms of Cyt b559 remain invariant up to a concentration of 200 μM and only the E_m value of HP Cyt b559 depends upon the herbicide concentration. At concentrations of dinoseb exceeding 200 μM, a partial transformation of the HP to the IP form is observed, while the level of the LP redox form remains unchanged. This

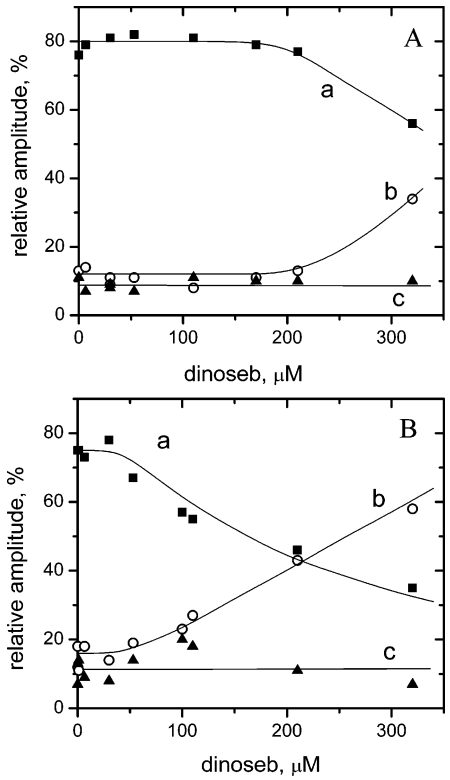

FIGURE 8: Relative amplitudes of HP (a), IP (b), and LP (c) forms of Cyt b559 as functions of the dinoseb concentration in suspensions of PS II membrane fragments preincubated anaerobically with dinoseb for 15 min (A) or 100 min (B) before the beginning of the redox titration. The relative amplitudes of the HP, IP, and LP Cyt b559 were gathered from titration experiments performed in samples containing different amounts of dinoseb. For further details, see the text and the Materials and Methods.

transformation is assumed to originate from a slow dinoseb-induced, most likely irreversible, structural change.

Figure 8B shows the relative amplitudes of HP, IP, and LP Cyt b559 gathered from redox titrations that were performed in samples preincubated for 100 min in the presence of dinoseb under anaerobic conditions. Oxygen was excluded to avoid autoxidation of HP Cyt b559 in the presence of dinoseb. The results reveal that under these conditions the onset of the HP to IP transformation of Cyt b559 is shifted to much lower concentrations of the herbicide. It is important to note that the E_m values of the Cyt b559 fraction that remains in the HP form in the sample preincubated with dinoseb were only slightly affected [the E_m values were lower by ~10−15 mV in the experiments of Figure 8B (not shown) as compared to those of Figure 8A (presented in part a of Figure 7)].

As it is illustrated in Figure 1, TPB, which is a powerful ionophoric PS II donor (*62*), leads to a similar dark oxidation of HP Cyt b559 as PS II herbicides DCMU and dinoseb. To address the possible influence of TPB on the E_m of Cyt b559, redox titrations of the heme protein were performed in PS II membrane fragments in the presence of TPB.

We have found in numerious redox titrations that the average E_m values of the IP and LP forms in most of our preparations of PS II membrane fragments from spinach and sugar beet cover ranges from +230 to +250 mV and from +50 to +120 mV, respectively (this paper and refs *36* and *55*). Some preparations, however, were characterized by lower midpoint potential values of the IP and LP forms of

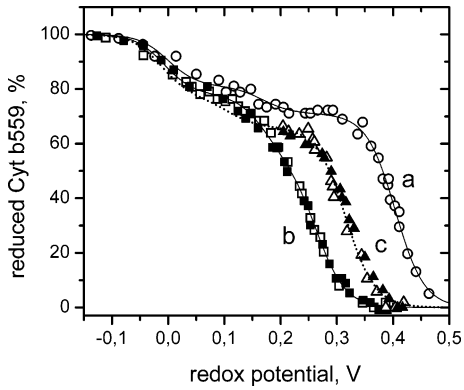

FIGURE 9: Relative amplitude of reduced Cyt b559 as a function of the redox potential in suspensions of PS II membrane fragments in the absence (a) and presence of either 30 μM TPB (b) or 20 μM CCCP (c). Open and closed symbols represent the data obtained in oxidative and reductive redox titrations, respectively. The best fit of the data points of the control sample a is a sum of three one-electron components with E_m values of +404, +169, and 0 mV and relative amplitudes of 71, 10, and 19%, respectively. The best fit for the data points of sample b is a sum of three one-electron components with E_m values of +265, +171, and −7 mV and relative amplitudes of 54, 24, and 22%, respectively. The best fit for the data points of sample c is a sum of three one-electron components with E_m values of +316, +107, and −12 mV and relative amplitudes of 66, 11, and 23%, respectively.

Cyt b559 with average E_m values of about +170 and 0 mV, respectively. In these preparations, the E_m value of IP Cyt b559 is similar to that reported by Losada and co-workers for PS II membrane-fragment preparations from spinach and pea leaves, where a redox form of Cyt b559 with an E_m value in the range from +140 to +200 mV has been found (*31*, *37*). It is important to note that, despite the variations in the E_m values of the IP and LP forms among the different PS II membrane-fragment preparations, the E_m value of the HP Cyt b559 (from +390 to +400 mV) is virtually invariant (this work and refs *36* and *55*).

The TPB-induced effect on E_m of HP Cyt b559 is markedly higher than that of the herbicides DCMU and dinoseb. Therefore, the preparations with the lower E_m values for the IP form provide the most suitable material to separate effects of TPB on the HP Cyt b559 from those induced in the IP form. Thus, this sample material was used for the titration experiments in the presence of TPB.

Figure 9 shows typical redox titration curves of Cyt b559 in the absence (curve a) and presence (curve b) of 30 μM TPB. An inspection of these data reveals two important phenomena: (i) the E_m of +404 mV for HP Cyt b559 observed in the control sample is shifted down to +265 mV in the presence of 30 μM TPB, while the values of E_m for IP and LP Cyt b559 remain unchanged, and (ii) the percentage of HP Cyt b559 decreases, accompanied by a concomitant increase in the amount of the IP form.

Figure 10 demonstrates that the midpoint potential of HP Cyt b559 exhibits a pronounced dependence on the concentration of TPB, while the redox potentials of the two other redox forms, IP and LP, do not deviate from the values determined in the absence of TPB. This feature is very similar to the redox titration patterns induced by DCMU and dinoseb.

An important result of Figure 10 is the finding that the E_m of the HP Cyt b559 reaches a plateau at high TPB

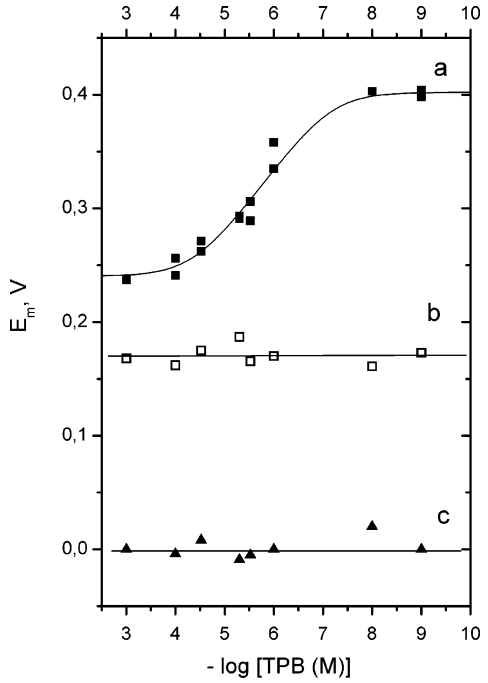

FIGURE 10: Midpoint potentials of HP (a), IP (b), and LP (c) redox forms of Cyt b559 as functions of the TPB concentration in suspensions of PS II membrane fragments. Redox titrations of Cyt b559 were performed in suspensions of PS II membrane fragments containing different amounts of TPB. The full-line curve for the data set (a) represents the best fit by eq 1 (see the Discussion) with the following parameters: $pK_{ox}^{TPB} = 7.14$, $pK_{red}^{TPB} = 4.4$, and E_m-([TPB] = 0) = +402 mV.

concentrations, thus indicating that saturation of the binding site with TPB takes place. As it is described in the Discussion, the fitting the data points by eq 1 leads to an asymptotic value of +237 mV for the E_m of HP Cyt b559 at high TPB concentrations. This value closely resembles typical values of E_m of the IP form. As a consequence of this similarity, an unambiguous separation between effects on HP and IP Cyt b559 cannot be achieved in investigations performed in most of our preparations. However, with the samples used for the experiments with TPB in this study, a clear distinction is possible between the HP form modified by TPB and the IP form.

Figure 11 depicts the relative content of the three redox forms as a function of the negative logarithm of the TPB concentration. These data reveal that, at TPB concentrations which are sufficiently low, the relative amounts of HP, IP, and LP Cyt b559 do not deviate from the values observed in untreated samples (with the E_m of HP Cyt b559 depending upon the TPB concentration). An analogous feature was observed also for DCMU and dinoseb as described above. Increasing TPB concentrations resulted in a marked increase in the relative amount of the IP form and, to a lesser extent, the LP form at the expense of the HP redox form. This finding indicates that high concentrations of TPB induce a transformation of the HP Cyt b559 into the IP and LP forms. A longer sample incubation in the presence of high TPB concentrations resulted in a pronounced increase of the percentage of LP Cyt b559 (data not shown). Therefore, reductive and oxidative redox titrations of Cyt b559 in the presence of 1 mM TPB were performed each in a new sample.

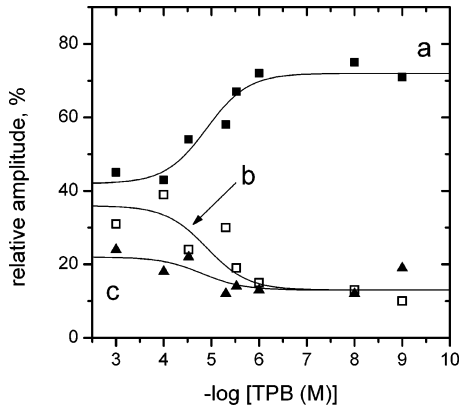

FIGURE 11: Relative amplitudes of HP (a), IP (b), and LP (c) forms of Cyt b559 as functions of the TPB concentration in suspensions of PS II membrane fragments. The relative amplitudes of the three redox forms of Cyt b559 were gathered from titration experiments performed in samples containing different amounts of TPB. For further details, see the text and the Materials and Methods.

The uncoupler and ADRY agent CCCP at a concentration of 15−30 μM was previously shown to promote the dark oxidation of HP Cyt b559, and the effect was assigned to a transformation of HP Cyt b559 to an autoxidizable LP form (*31*). This explanation, however, appears to be questionable when taking into consideration similar effects of DCMU, dinoseb, and TPB on HP Cyt b559. To address this point, we have examined the redox pattern of HP Cyt b559 in the presence of CCCP. The results obtained (curve c in Figure 9) show that in the presence of 20 μM CCCP the E_m of HP Cyt b559 significantly decreases to a value of +316 mV, while the relative content of this redox form is diminished by only 5%. This finding is a clear indication for the effect of CCCP on the redox pattern of Cyt b559 being qualitatively identical to that induced by DCMU, dinoseb, and TPB. Accordingly, a common mechanism is responsible for the action on HP Cyt b559 of all of the compounds studied in the present work.

DISCUSSION

Mechanism of the Dark Oxidation of HP Cyt b559. The present paper describes effects of the PS II herbicides DCMU and dinoseb, the powerful ionophoric PS II donor TPB, and the ADRY compound CCCP on the redox properties of Cyt b559. We have shown that three of the studied compounds, DCMU, dinoseb, and TPB, induced the dark oxidation of HP Cyt b559 in preparations of PS II membrane fragments. In earlier studies, the ADRY reagents CCCP, FCCP, and Ant2p (*31*, *41*, *56*, *69*, *70*), the phenolic herbicide dinoseb (*71*), and TPB (*67*) were also reported to induce the dark oxidation of HP Cyt b559, and the effect was interpreted as to originate from a HP → LP transformation of Cyt b559. However, this explanation is not straightforward because it lacks the sound basis of detailed redox titration experiments.

Therefore, thorough examinations on the redox titration pattern of Cyt b559 were performed in the presence of DCMU, dinoseb, TPB, and CCCP. The data obtained revealed for the first time that in a selected concentration range of the active substances (this range depends upon the nature of the compound) an autoxidation of Cyt b559 can

Scheme 1: Schematic Representation of the Interaction of Exogenous Substances L Bound at Site Q_C and HP Cyt b559[a]

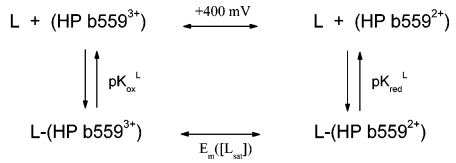

[a] The symbol $E_m([L_{sat}])$ describes the midpoint potential of HP Cyt b559 when the binding of L reaches the saturation level (for details, see the text).

be induced without any concomitant transformation of the HP Cyt b559 into the IP and/or LP form(s) (compare Figure 1 to Figures 5, 8A, and 11). In excellent correspondence with this result, dark oxidation of HP Cyt b559 in the presence of DCMU was found to be completely prevented if the ambient redox potential of the suspension is buffered at 300 mV (see Figure 2). Furthermore, DCMU, dinoseb, and TPB specifically decreased the midpoint potential of HP Cyt b559 in a concentration-dependent manner, accompanied neither by analogous effects on the E_m of IP and LP Cyt b559 nor by a marked transformation of HP Cyt b559 into the IP or LP forms (see Figures 4−11).

The results gathered from the data of the present study lead to the following conclusions: (i) the PS II complex contains a binding site for DCMU, dinoseb, TPB, and CCCP, symbolized by Q_C, which exhibits an interaction (direct or remote) with the heme group of Cyt b559; (ii) among the three discernible forms of Cyt b559 (HP, IP, and LP), these interactions are restricted to the heme group of HP Cyt b559; and (iii) the binding of an active substance at the Q_C site is dependent upon the redox state of HP Cyt b559, with a higher affinity when the heme group is oxidized.

Potentiometric effects on the heme group induced by herbicides are an entirely new phenomenon for HP Cyt b559 in PS II, but analogous effects were already reported in the literature for other b-type cytochromes. Various Q-site inhibitors are known to affect the E_m values of b-type hemes in different quinone/quinol-dependent oxidoreductases. For instance, the binding of inhibitors to sites Q_o and Q_i of the bc_1 complex causes various shifts of the E_m values of hemes b_L and b_H (*82*−*84*). In succinate:menaquinone oxidoreductase from *Bacillus subtilis*, occupation by the quinone analogue 2-*n*-heptyl 4-hydroxyquinoline-*N*-oxide (HOQNO) of a quinone-binding site induces a negative shift of about 60 mV in E_m of the interacting heme b_L (*85*). Substantial potentiometric effects are also reported for the diheme b-type cytochrome of *Escherichia coli* nitrate reductase A because of the binding of the inhibitors HOQNO and stigmatellin (*86*).

The effect on the E_m of HP Cyt b559 induced by the binding of DCMU, dinoseb, TPB, and CCCP to the presumed Q_C site can be explained within the framework of a general scheme originally considered by Clark (*87*) (see also ref *88*). The essential point of this mechanism is the idea that the binding affinity of a substance to a redox protein depends upon the oxidation state of its integral redox group(s). Scheme 1 illustrates this mechanism.

Table 1: Dissociation Constants in the Q_C Site for Some PS II Inhibitors Determined by their Effect on the E_m of HP Cyt b559 [nd = Not Determined (See the Text)]

	pK_{ox}	pK_{red}
DCMU	3.70	nd
dinoseb	5.18	nd
TPB	7.14	4.40

Accordingly, the midpoint redox potential of HP Cyt b559 in the presence of a compound L (in our case, DCMU, dinoseb, TPB, or CCCP) at concentration [L], $E_m([L])$, is given by the following equation:

$$E_m([L]) = E_m([L] = 0) + \frac{RT}{nF}\ln\frac{(1 + [L]/K_{red}^{L})}{(1 + [L]/K_{ox}^{L})} \quad (1)$$

where K_{ox}^{L} and K_{red}^{L} are the dissociation constants of the compound L in the Q_C site when the heme group of HP Cyt b559 is oxidized and reduced, respectively. In eq 1, [L] denotes the concentration of free, i.e., unbound, compound L, so that

$$[L] = [L_o] - [L\text{-}Q_C] \quad (2)$$

where $[L_o]$ is the total concentration of L and $[L\text{-}Q_C]$ is the concentration of PS II centers with a Q_C site occupied by compound L. The data presented in Figures 4a, 7a, and 10a were analyzed by using eq 1 and the approximation

$$[L] \approx [L_o] \quad (3)$$

which is satisfied for $[L\text{-}Q_C] \ll [L_o]$. The concentration of PS II complexes used in titration experiments of the present study was about 0.2 μM, and this value determines the upper limit for $[L\text{-}Q_C]$. Therefore, the use of the relation (eq 3) is well-justified for fitting the data points by eq 1 for $[L_o] \geq 2$ μM ($p[L] \leq 5.7$). On the other hand, at concentrations of $[L_o]$ approaching 0, the ratios $[L_o]/K_{ox}^{L}$ and $[L_o]/K_{red}^{L}$ are very small and can be neglected, so that the $E_m([L])$ values approaches a limit $E_m([L] = 0)$ as experimentally observed. The use of eq 1 tacitly implies that the kinetics of L equilibration with Q_C is fast compared with the redox titration (about 2−3 min for each data point).

The pK^{L} values gathered from the fits of the experimental data for DCMU, dinoseb, and TPB are summarized in Table 1. The $E_m([L] = 0)$ value is about +400 mV as determined for HP Cyt b559 in untreated PS II samples, while a value of about +240 mV for $E_m([L_{sat}])$ was obtained from the data of Figure 10 as the asymptotic value that is reached at TPB concentrations sufficiently higher than K_{red}. For the two herbicides DCMU and dinoseb, the second inflection point of the curves of the E_m of HP Cyt b559 as a function of $p[L](-\log([L]))$ has not been reached within the region of the L concentrations covered in the present study. As a consequence, the precise values of pK_{red}^{DCMU} and pK_{red}^{dino} for the herbicide affinity of the Q_C site could not be determined in the case of reduced HP Cyt b559 and fitting the data points in Figures 4a and 7a was done by assuming reasonable values of pK_{red}^{L} (see the captions of Figures 4 and 7).

The mechanism described by Scheme 1 implies that remarkable structural differences exist between the oxidized and reduced states of HP Cyt b559, which determine the

difference of the binding constants, ΔpK^L, of the Q_C site. The existence of structural differences between oxidized and reduced forms of HP Cyt b559 has been already reported in the literature (*31*, *32*, *36*, *54*). We suggested, on the basis of investigations of optical oxidized minus reduced difference spectra of Cyt b559, that a spin-state transition of the heme iron takes place upon redox change of the heme group in HP Cyt b559 (*36*). In marked contrast to HP Cyt b559, analogous spectral peculiarities were not observed for the IP and LP forms of Cyt b559. These results complement nicely the findings of the present study and support the idea of a redox-dependent structural rearrangement in the vicinity of the heme group of Cyt b559 that is specific for the HP form.

Scheme 1 explains the autoxidation of HP Cyt b559 in the presence of a substance L (in the present study, DCMU, dinoseb, TPB, or CCCP) at concentrations that cause only slight down shifts of E_m, e.g., in the presence of 320 μM DCMU or micromolar concentrations of dinoseb. Autoxidation of HP Cyt b559 induced by low concentrations of L occurs via a small transiently populated fraction of PS II complexes with reduced HP Cyt b559 and a Q_C site occupied by L. In this fraction of the HP Cyt b559 with bound L, the redox potential of the heme group attained the value of E_m-([L_{sat}]). The rate and extent of net autoxidation of HP Cyt b559 induced by different concentrations of L are governed by the steady-state concentration of complexes HP Cyt $b559^{red}$−L and the ambient redox potential of the suspension.

The Q_C Site Is Different from the Q_B Site. The results of the present study lead to the conclusion that a binding site Q_C exists for exogenous substances, which is characterized by special properties, i.e., the dependence of its binding affinity on the redox state of HP Cyt b559. Therefore, questions arise on the nature of this site. It has been reported that the ADRY agent CCCP may be able to occupy the Q_B site (*78*, *89*, *90*) and to compete with DCMU in binding to this site (*78*). At first glance, this finding and the effect of ADRY compounds on the redox properties of Cyt 559 together with the relative proximity of the heme group to the Q_B site (*18*−*23*) might suggest that binding L to this site could also induce the effects on Cyt b559. However, on the basis of our results, this possibility can be definitely ruled out for several reasons.

First, the DCMU binding at the Q_B site with a value of K_{DCMU} in the range of 15−40 nM (*75*−*79*) and at the Q_C site with a value of $K_{ox}^{DCMU} = 200$ μM gathered from a fit of the DCMU effect on the E_m of HP Cyt b559 (present study, see Table 1) differ by a factor of more than 1000. Second, the binding affinity of DCMU to the Q_B site was not reported to be dependent upon the redox state of Cyt b559. In fact, the affinity constants for DCMU at the Q_B site determined either by the equilibrium binding of the labeled herbicide to thylakoids in the dark (in this case, HP Cyt b559 is kept reduced) or by oxygen evolution measurements in the presence of the electron acceptor $K_3[Fe(CN)_6]$ (i.e., when HP Cyt b559 is oxidized) were found to be very similar (*75*−*79*). Third, the occupancy by DCMU of the Q_B site has no effect on the redox titration pattern of Cyt b559 in the presence of dinoseb (see Figure 7). The latter fact indicates that neither the binding affinity of dinoseb to the Q_C site nor the number of dinoseb-binding Q_C sites were changed when a DCMU molecule was bound in the Q_B site. This finding unambiguously shows that Q_B and Q_C are different sites in the PS II structure.

Interpretation of the Data on Interactions of PS II with Herbicides within the Framework of Q_B and Q_C Sites. Our conclusion on the existence of a site Q_C in addition to Q_B offers a new insight into experimental data obtained for the interaction of various herbicides with PS II, which are not easily understandable within the framework of a single common binding site for all PS II herbicides. These findings comprise the noncompetitive behavior in affinity studies of some pairs of herbicides (*80*, *91*, *92*), the complex displacement behavior between different PS II herbicides (*80*, *93*, *94*), puzzling results gathered from photoaffinity-labeling studies, which show the binding of herbicides to the PS II complex when the Q_B site is already occupied by a covalently linked compound (*95*−*97*), and the opposite sensitivity to different classes of PS II herbicides of several mutants, where amino acids at or near the Q_B pocket are replaced by other residues through site-directed mutagenesis (*76*, *92*, *94*, *98*−*101*).

A very illustrative example for the complex character of herbicide interactions with PS II is the marked differences between effects caused by "classical" and phenolic-type herbicides (reviewed in refs *6*, *7*, and *9*−*12*). These differences include several properties: (i) association/dissociation kinetics for inhibitor binding (*78*, *79*, *81*, *102*), (ii) susceptibility of PS II toward photoinhibition in the presence of these herbicides (*103*−*111*), (iii) effects on the redox potential of $Q_A/Q_A^{-\cdot}$ (*110*) and on electron paramagnetic resonance (EPR) signals of the non-heme iron (*11*), (iv) properties in trypsin-treated chloroplasts (*80*, *91*, *112*−*120*), and (v) light-induced Car oxidation (*71*, *121*). These striking differences between the effects of "classical" and phenolic herbicides are difficult to understand if these compounds are bound exclusively to the Q_B site in PS II.

Some of the differences could be rationalized by the assumption that urea, triazine, quinone, and phenolic herbicides interact with different amino acid residues in the Q_B-binding niche (*76*, *80*, *94*, *95*, *100*, *122*, *123*). Furthermore, the opposite effects of "classical" and phenolic herbicides on the $Q_A/Q_A^{-\cdot}$ redox potential were explained by electrostatic interaction of $Q_A^{-\cdot}$ with the bound phenolic herbicide anion (*110*) and/or by assuming various conformational changes in the Q_A-Q_B protein domain because of a different mode of binding of herbicides to the Q_B niche (*110*, *123*).

An alternative and straightforward interpretation of some puzzling data, however, can be offered by our proposal on the existence of two binding sites for herbicides within the PS II complex (Q_B and Q_C sites). It appears reasonable to suggest that some effects specifically induced by phenolic herbicides originate from their simultaneous binding to both the Q_B and Q_C sites because of their similar binding affinity. In this respect, it is most interesting to note that the effects, which are specific for phenolic herbicides and not observed for "classical" herbicides (at least at concentrations saturating the binding to the Q_B site) resemble those of ADRY compounds. These effects include the enhancement of dark- and light-induced oxidation of Cyt b559 (this paper and refs *15*, *31*, *41*, *56*, and *64*−*71*), the induction of Car photooxidation (*67*, *71*, *121*, *124*, *125*), and the drastically increased

decay rates of the redox states S_2 and S_3 of the WOC (*57*−*60*, *93*, *123*, *126*). The results of the present paper are in excellent correspondence with these findings and highly support the idea of a common binding site for phenolic herbicides and ADRY compounds in the PS II complex that is different from the Q_B site. In an analysis of the strikingly similar effects of diphenylamines and ADRY-type reagents in PS II, Oettmeier and Renger suggested that the main action site of diphenylamines is the protein moiety of Cyt b559 (*93*). It seems likely that the negative charge of the anionic form of ADRY compounds and phenolic herbicides at physiological pH values is important for their binding properties at the Q_C site.

The idea of the existence of two herbicide binding sites with different affinities is supported by equilibrium binding studies on atrazine (*127*, *128*) and other herbicides (*101*) and results gathered from photoaffinity-labeling investigations, which identified the binding to proteins of 28−34 and 41−53 kDa (*81*, *91*, *99*, *101*, *129*, *130*). A low-affinity site for atrazine has also been identified on the basis of an antibody-binding analysis (*128*). Furthermore, it has been suggested that a second site of herbicide action is located on the donor side of the PS II complex (*131*−*134*).

Cyt b559−Q_C *Interactions and the Physiological Role of the* Q_C *Site*. The reagents that were found to interact with the proposed Q_C site (PS II herbicides, ADRY compounds, and TPB) also bind to the Q_B niche. As a consequence, it appears likely that the Q_C site is also a PQ-exchangeable domain of PS II, which interacts with PQ/PQH_2. This conclusion is in line with the results of a recent study (*44*) where the existence in PS II of two further PQ-binding sites, besides Q_A and Q_B, has been proposed. However, unlike the previous assumption on the PQ interaction with LP Cyt b559 (*44*), our investigation suggests that the PS II complex contains a PQ-binding site (Q_C) when Cyt b559 is in the HP form.

The affininty of all endogenous compounds L tested in the present study strongly depends upon the redox state of HP Cyt b559. This finding suggests the possibility that the redox state of the heme group also regulates the Q_C-site affinity to the native components PQ and PQH_2. Accordingly, the binding of PQ cofactors to the Q_C site is assumed to induce a shift in the E_m of Cyt b559.

The key proposal of our model is the assumption that the binding of PQ to the Q_C site is essential in establishing a high (+400 mV) midpoint potential of the heme group in Cyt b559. This conclusion is based on earlier findings on a decrease of the relative content of HP Cyt b559 upon PQ extraction from lyophilized chloroplast preparations by hexane or heptane washing (*51*, *135*, *136*) and subsequent dark restoration of the HP form to levels of 50−70% of the control after the supplementation of samples with PQ (*136*).

The extent of HP Cyt b559 depends upon the sample type. In the case of PS II preparations from higher plants, the HP form of Cyt b559 becomes missing at the structural hierarchy level of PS II core complexes (*36*), i.e., after deprivation of the natural membrane environment. In PS II core complexes from the thermophilic cyanobacterium *T. elongatus*, the HP form of Cyt b559 is lacking in the preparation of a high degree of purification that is necessary to obtain 3D crystals for X-ray diffraction studies of sufficient resolution (*55*). On the other hand, HP Cyt b559 is partially retained in a presumably less purified preparation from *T. elongatus* (*137*).

To account for the effect of PQ on the E_m of Cyt b559, we assume that the binding of PQ to the Q_C site stabilizes the reduced form of Cyt b559. As a consequence, the affinity of Q_C to PQ is much higher in the reduced HP Cyt b559 as compared to the oxidized form, i.e., $pK_{red}^{PQ} > pK_{ox}^{PQ}$. It is important to point out that we consider equilibrium binding of an exchangeable PQ molecule at the Q_C site, which implies the existence of a "PQ-free" form of Cyt b559 that is characterized by a lower midpoint potential of the heme group and different conformations of its microenvironment in the oxidized and reduced state. This presumed "PQ-free" Cyt b559 form, which retains a protein configuration specific for the HP form, will be denoted as the intermediate (IM) form to distinguish it from the known IP and LP forms. These latter forms are believed to lack the propensity to undergo a specific conformational change upon oxidoreduction of the heme group characteristic of HP Cyt b559 (*31*, *32*, *36*, *48*, *54*).

The IM form is considered to be unstable. Thus, the occupancy of the Q_C site by PQ can be regarded as a factor preserving a specific protein conformation that is characteristic of the HP Cyt b559. Within the framework of this model, the transformation of HP Cyt b559 to the IP and LP forms by various treatments (sonication, aging, heating, and incubation with detergents, salts, or at high and low pH) originates from a depletion of the Q_C site from the bound PQ, followed by further conformational rearrangements of the unstable IM form, thus, leading to the population of IP and LP Cyt b559. This idea is highly supported by the experimental finding that the stability toward different sample treatments is significantly higher for reduced than oxidized HP Cyt b559 (*31*, *34*, *36*, *54*).

The results of the present investigation corroborate the conclusion on the instability of the "PQ-depleted" HP Cyt b559. A gradual shift in the E_m of HP Cyt b559 because of increasing concentrations of PS II inhibitors (Figures 4a, 7a, and 10a) is indicative of a dynamic equilibrium process described by Scheme 1. Accordingly, a regeneration of HP Cyt b559 (E_m of +400 mV) is expected when the exogenous cofactor L is replaced by PQ in the Q_C site. The data of this study show that an irreversible transformation HP → IP (LP) takes place (Figures 8 and 11) when the Q_C site is nearly saturated with TPB or dinoseb, i.e., at $[L] \geq K_{red}^{L}$; at lower concentrations of L, longer incubation times are required to evoke this effect. On the basis of the postulated interaction between Cyt b559 and PQ, these findings are explained by the instability of a protein configuration characteristic of HP Cyt b559 in the "PQ-free" form.

Our results and data from the literature do not provide information on the exact E_m value of the "PQ-free" HP Cyt b559 (IM form). In the PQ extraction experiments on chloroplasts, the "PQ-depleted" Cyt b559 form, which was able to restore the high E_m value of the HP form by equilibrium binding of PQ, was reported to not be reducible by hydroquinone (*136*). This study, however, was significantly complicated by an obvious instability of the HP Cyt b559 in the PQ-free IM form.

On the basis of the proposed interaction between PQ and HP Cyt b559, the effect on its E_m induced by exogenous

compounds comprises the replacement of PQ at the Q_C site by L. In the case of TPB, a value of about +240 mV was determined for $E_m([L_{sat}])$ (Figure 10). For DCMU and dinoseb, the maximal values for $E_m([L_{sat}])$ leading to satisfying fits of the observed slope of the curves in Figures 4a and 7a were estimated to be +290 and +190 mV, respectively. Correspondingly, any lower value for $E_m([L_{sat}])$ is also equally suitable. The chemical structure of the compounds tested in the present study is quite different; in particular, TPB does not contain any N and O atoms, which can form relatively strong hydrogen bonds with the protein environment. On the other hand, the ligating native PQ is expected to be linked through hydrogen bonds with amino acids in the Q_C site. As a consequence, the binding interaction between TPB and the protein interior of the IM form is probably not greatly influenced by a change in the redox state of the heme group; i.e., pK_{red} and pK_{ox} are nearly the same for the binding of TPB with the IM form. Therefore, it seems likely that the main contribution to the negative E_m shift of HP Cyt b559 induced by TPB originates from a release of bound PQ rather than the binding of TPB. This would imply a value of +240 mV as a rough estimate for the E_m of the IM form of Cyt b559, corresponding to a value of 2.7 for the difference in the binding affinity, $\Delta pK = pK_{red} - pK_{ox}$, of PQ with the Q_C site of the IM form, in the case of the reduced and oxidized heme groups, respectively.

An intriguing question is on the possible role of the Q_C site in the function of PS II. It has been suggested that Cyt b559 may participate in the oxidation of PQH_2 by molecular oxygen (*43*−*45*), and the LP form of Cyt b559 was assumed to mediate the PQH_2 oxidation (*43*). These considerations are in line with the idea that a reversible transition HP ↔ LP is essential for the protective function of Cyt b559 *in vivo* (*31*, *46*, *138*−*140*). The complete reduction of the electron acceptors Q_A and Q_B was considered to be a factor that induces the transformation of HP Cyt b559 to an LP form (*138*). Although the results of the present study are fully consistent with this static view, the general problem emerging from this proposal is the nature of the underlying mechanism that provides reversibility of the presumed HP ↔ LP transition. On the other hand, the idea of E_m regulation by binding the PQ cofactor at the Q_C site offers an alternative and more elegant mechanism for the role of Cyt b559 in the protection from photoinhibition.

The assumption of reduced Cyt b559 in the specific protein configuration, IM, being capable of a preferential binding of PQ (thus shifting the E_m of the heme to +400 mV) also implies the possibility of a reversed order in the affinity of Q_C to PQH_2. If PQH_2 preferentially binds when IM Cyt b559 is oxidized, the occupancy of Q_C by PQH_2 would induce a negative shift in the E_m of Cyt b559 as compared to the E_m of the IM form. The opposite binding affinity of PQ and PQH_2 to the Q_C site in the reduced and oxidized IM forms can be rationalized by the assumption that the structural rearrangements in the site are minimal during the course of oxidoreduction of the heme group, but the redox transition is coupled to a change in the protonation pattern of amino acid residues acting as ligands for bound PQ. This mechanism would provide a significant and fully reversible shift in the E_m of the Cyt b559 heme group simply by changing the redox state of the PQ molecule bound at the Q_C site. Such a mode of interaction would allow for a switch between the function of Cyt b559 acting as a protectant either to the donor- or acceptor-side photoinhibitions, depending upon the overall rate of the photosynthetic electron flow and the level of reduction of the PQ pool.

Q_C Site Hypothesis and Structural Data. A direct proof for the existence and exact localization of the putative Q_C site in PS II would be its identification by a high-resolution X-ray structure. The unravelling of quinone-binding sites is an ambituous goal. Until recently, information on the Q_B site was rather poor. A breakthrough, however, was achieved when the resolution of the X-ray crystal structure of PS II core complexes from *T. elongatus* could be improved to 3.0 Å (*23*). One striking feature of the novel structure is the discovery of a large cavitiy with two openings: one toward the cytoplasmic side and a smaller one toward the membrane interior. The large lipophilic cavity possibly provides a pathway for the diffusion of PQ. With respect to the conclusions of the present study, the smaller opening of the cavity is of special interest. It is flanked by the transmembrane helices (TMHs) of the subunits PsbE and PsbF of Cyt b559 as well as the TMH of PsbJ and is also in close contact with the heme group. These structural peculiarities favor an interaction between the PQ/PQH_2 of the pool and the heme group of Cyt b559. Therefore, the currently available structural data of highest resolution (*23*) are in favor of the idea of a PQ/PQH_2-binding site near Cyt b559. New X-ray data of higher resolution on crystals that retain the HP form of Cyt b559 are required to elucidate the structure of a presumed Q_C site.

CONCLUDING REMARKS

The present study has shown that a hitherto unknown domain exists in PS II that is assigned to a quinone-binding pocket at HP Cyt b559 or in its vicinity. The affinity of this domain, denoted as the Q_C site, to exogenous substances (PS II herbicides, TPB, and also "true" ADRY agents) depends specifically upon the redox state of the heme group of HP Cyt b559. We propose that the interaction between the heme group and the Q_C site occupied by a PQ molecule gives rise to the unique properties of HP Cyt b559, which is characterized by an unusually high redox potential. A regulation of the E_m of Cyt b559 by the ratio PQ/PQH_2 of the pool via the Q_C site may ensure a switch between functional redox forms of Cyt b559 and provide a mechanism of protection of PS II from photoinhibition.

ACKNOWLEDGMENT

We thank Drs. A. Zouni, K.-D. Irrgang, and J. Kern for stimulating discussions on the PS II structure. The financial supports by grants from the Russian Fund of Basic Research (05-04-49488) and DFG (436 Rus 113/635/0-1) are gratefully acknowledged.

REFERENCES

1. Ke, B. (2001) *Photosynthesis: Photobiochemistry and Photobiophysics*, Kluwer Academic Publishers, Dordrecht, The Netherlands.
2. Debus, R. J. (1992) The manganese and calcium ions of photosynthetic oxygen evolution, *Biochim. Biophys. Acta 1102*, 269−352.
3. Renger, G. (1997) Photosystem II and water oxidation in cyanobacteria, algae and higher plants, in *Treatise on Bioelectrochem-*

istry (Gräber, P., and Milazzo, G., Eds.) Birkhäuser, Basel, Switzerland, Vol. 2: Bioenergetics, pp 310−358.
4. Renger, G., and Holzwarth, A. R. (2005) Primary electron transfer, in *Photosystem II: The Water/Plastoquinone Oxido-reductase in Photosynthesis* (Wydrzynski, T., and Satoh, K., Eds.) Kluwer Academic Publishers, Dordrecht, The Netherlands, pp 139−175.
5. Petrouleas, V., and Crofts, A. R. (2005) The iron−quinone acceptor complex, in *Photosystem II: The Water/Plastoquinone Oxido-reductase in Photosynthesis* (Wydrzynski, T., and Satoh, K., Eds.) Kluwer Academic Publishers, Dordrecht, The Netherlands, pp 177−206.
6. Trebst, A. (1980) Inhibitors in electron flow: Tools for the functional and structural localization of carriers and energy conservation sites, *Methods Enzymol. 69*, 675−715.
7. Vermaas, W. F. J., and Govindjee (1981) The acceptor side of photosystem II in photosynthesis, *Photochem. Photobiol. 34*, 775−793.
8. Crofts, A. R., and Wraight, C. A. (1983) The electrochemical domain of photosynthesis, *Biochim. Biophys. Acta 726*, 149−185.
9. Renger, G. (1986) Herbicide interaction with PS II: Recent developments, *Physiol. Veg. 24*, 509−521.
10. Trebst, A., and Draber, W. (1986) Inhibitors of photosystem II and the topology of the herbicide and Q_B binding polypeptide in the thylakoid membrane, *Photosynth. Res. 10*, 381−392.
11. Diner, B. A., Petrouleas, V., and Wendoloski, J. J. (1991) The iron−quinone electron-acceptor complex of photosystem II, *Physiol. Plant. 81*, 423−436.
12. Oettmeier, W. (1999) Herbicide resistance and supersensitivity in photosystem II, *Cell. Mol. Life Sci. 55*, 1255−1277.
13. Yachandra, V. K., Sauer, K., and Klein, M. P. (1996) Manganese cluster in photosynthesis: Where plants oxidize water to dioxygen, *Chem. Rev. 96*, 2927−2950.
14. Renger, G. (2001) Photosynthetic water oxidation to molecular oxygen: Apparatus and mechanism, *Biochim. Biophys. Acta 1503*, 210−228.
15. Cramer, W. A., and Whitmarsh, J. (1977) Photosynthetic cytochromes, *Ann. Rev. Plant Physiol. 28*, 133−172.
16. Whitmarsh, J., and Pakrasi, H. B. (1996) Form and function of cytochrome b-559, in *Oxygenic Photosynthesis: The Light Reactions* (Ort, D. R., and Yocum, C. F., Eds.) Kluwer Academic Publishers, The Netherlands, Dordrecht, pp 249−264.
17. Stewart, D. H., and Brudvig, G. W. (1998) Cytochrome b_{559} of photosystem II, *Biochim. Biophys. Acta 1367*, 63−87.
18. Zouni, A., Witt, H.-T., Kern, J., Fromme, P., Krauss, N., Saenger, W., and Orth, P. (2001) Crystal structure of photosystem II from *Synechococcus elongatus* at 3.8 Å resolution, *Nature 409*, 739−743.
19. Kamiya, N., and Shen, J.-R. (2003) Crystal structure of oxygen-evolving photosystem II from *Thermosynechococcus vulcanus* at 3.7 Å resolution, *Proc. Natl. Acad. Sci. U.S.A. 100*, 98−103.
20. Ferreira, K. N., Iverson, T. M., Maghlaoui, K., Barber, J., and Iwata, S. (2004) Architecture of the photosynthetic oxygen-evolving center, *Science 303*, 1831−1838.
21. Biesiadka, J., Loll, B., Kern, J., Irrgang, K.-D., and Zouni, A. (2004) Crystal structure of cyanobacterial photosystem II at 3.2 Å resolution: A closer look at the Mn-cluster, *Phys. Chem. Chem. Phys. 6*, 4733−4736.
22. Kern, J., Loll, B., Zouni, A., Saenger, W., Irrgang, K.-D., and Biesiadka, J. (2005) Cyanobacterial photosystem II at 3.2 Å resolution−The plastoquinone binding pockets, *Photothynth. Res. 84*, 153−159.
23. Loll, B., Kern, J., Saenger, W., Zouni, A., and Biesiadka, J. (2005) Towards complete cofactor arrangement in the 3.0 Å resolution structure of photosystem II, *Nature 438*, 1040−1044.
24. Herrmann, R. G., Alt, J., Schiller, B., Widger, W. R., and Cramer, W. A. (1984) Nucleotide sequence of the gene for apocytochrome b-559 on the spinach plastid chromosome: Implications for the structure of the membrane protein, *FEBS Lett. 176*, 239−244.
25. Widger, W. R., Cramer, W. A., Hermodson, M., and Herrmann, R. G. (1985) Evidence for a hetero-oligomeric structure of the chloroplast cytochrome b-559, *FEBS Lett. 191*, 186−190.
26. Babcock, G. T., Widger, W. R., Cramer, W. A., Oertling, W. A., and Metz, J. G. (1985) Axial ligands of chloroplast cytochrome b-559: Identification and requirement for a heme-cross-linked polypeptide structure, *Biochemistry 24*, 3638−3645.
27. Tae, G. S., Black, M. T., Cramer, W. A., Vallon, O., and Bogorad, L. (1988) Thylakoid membrane protein topography: Transmembrane orientation of the chloroplast cytochrome b-559 psbE gene product, *Biochemistry 27*, 9075−9080.
28. Tae, G. S., and Cramer, W. A. (1989) Lumen-side topography of the α-subunit of the chloroplast cytochrome b-559, *FEBS Lett. 259*, 161−164.
29. Tae, G. S., and Cramer, W. A. (1992) Truncation of the COOH-terminal domain of the psbE gene product in *Synechocystis* sp. PCC 6803: Requirements for photosystem II assembly and function, *Biochemistry 31*, 4066−4074.
30. Tae, G. S., and Cramer, W. A. (1994) Topography of the heme prosthetic group of cytochrome b-559 in the photosystem II reaction center, *Biochemistry 33*, 10060−10068.
31. Ortega, J. M., Hervas, M., and Losada, M. (1988) Redox and acid-base characterization of cytochrome b-559 in photosystem II particles, *Eur. J. Biochem. 171*, 449−455.
32. Thompson, L. K., Miller, A.-F., Buser, C. A., de Paula, J. C., and Brudwig, G. W. (1989) Characterization of the multiple forms of cytochrome b_{559} in photosystem II, *Biochemistry 28*, 8048−8056.
33. Shuvalov, V. A., Schreiber, U., and Heber, U. (1994) Spectral and thermodynamic properties of the two hemes of the D1D2cytochrome b-559 complex of spinach, *FEBS Lett. 337*, 226−230.
34. McNamara, V. P., and Gounaris, K. (1995) Granal photosystem II complexes cotain only the high redox potential form of cytochrome b-559 which is stabilised by the ligation of calcium, *Biochim. Biophys. Acta 1231*, 289−296.
35. Iwasaki, I., Tamura, N., and Okayama, S. (1995) Effects of light stress on redox potential forms of Cyt b-559 in photosystem II membranes depleted of water-oxidizing complex, *Plant Cell Physiol. 36*, 583−589.
36. Kaminskaya, O., Kurreck, J., Irrgang, K.-D., Renger, G., and Shuvalov, V. A. (1999) Redox and spectral properties of cytochrome b_{559} in different preparations of photosystem II, *Biochemistry 38*, 16223−16235.
37. Roncel, M., Ortega, J. M., and Losada, M. (2001) Factors determining the special redox properties of photosynthetic cytochrome b559, *Eur. J. Biochem. 268*, 4961−4968.
38. Whitmarsh, J., and Cramer, W. A. (1978) A pathway for the reduction of cytochrome b-559 by photosystem II in chloroplasts, *Biochim. Biophys. Acta 501*, 83−93.
39. Böhme, H., and Kunert, K.-J. (1980) Photoreactions of cytochromes in algal chloroplasts, *Eur. J. Biochem. 106*, 329−336.
40. Tsujimoto, H. Y., and Arnon, D. I. (1985) Differential inhibition by plastoquinone analogues of photoreduction of cytochrome b-559 in chloroplasts, *FEBS Lett. 179*, 51−54.
41. Arnon, D. I., and Tang, G. M.-S. (1988) Cytochrome b-559 and proton conductance in oxygenic photosynthesis, *Proc. Natl. Acad. Sci. U.S.A. 85*, 9524−9528.
42. Buser, C. A., Diner, B. A., and Brudvig, G. W. (1992) Photooxidation of cytochrome b_{559} in oxygen-evolving photosystem II, *Biochemistry 31*, 11449−11459.
43. Kruk, J., and Strzalka, K. (1999) Dark reoxidation of the plastoquinone-pool is mediated by the low-potential form of cytochrome b-559 in spinach thylakoids, *Photosynth. Res. 62*, 273−279.
44. Kruk, J., and Strzalka, K. (2001) Redox changes of cytochrome b_{559} in the presence of plasoquinones, *J. Biol. Chem. 276*, 86−91.
45. Bondarava, N., de Pascalis, L., Al-Babili, S., Goussias, C., Golecki, J. R., Beyer, P., Bock, R., and Krieger-Liszkay, A. (2003) Evidence that cytochrome b_{559} mediates the oxidation of reduced plastoquinone in the dark, *J. Biol. Chem. 278*, 13554−13560.
46. Butler, W. L. (1978) On the role of cytochrome b_{559} in oxygen evolution in photosynthesis, *FEBS Lett. 95*, 19−25.
47. Desbois, A., and Lutz, M. (1992) Redox control of proton transfers in membrane b-type cytochromes: An absorption and resonance Raman study on bis(imidazole) and bis(imidazolate) model complexes of iron−protoporphyrin, *Eur. Biophys. J. 20*, 321−335.
48. Berthomieu, C., Boussac, A., Mantele, W., Breton, J., and Nabedryk, E. (1992) Molecular changes following oxidoreduction of cytochrome b559 characterized by Fourier transform infrared difference spectroscopy and electron paramagnetic resonance: Photooxidation in photosystem II and electrochemistry of isolated cytochrome b559 and iron protoporphyrin IX-bisimidazole model compounds, *Biochemistry 31*, 11460−11471.
49. Krishtalik, L. I., Tae, G. S., Cherepanov, D. A., and Cramer, W. A. (1993) The redox properties of cytochromes b imposed by the membrane electrostatic environment, *Biophys. J. 65*, 184−195.
50. Wada, K., and Arnon, D. I. (1971) Three forms of cytochrome b559 and their relation to the photosynthetic activity of chloroplasts, *Proc. Natl. Acad. Sci. U.S.A. 68*, 3064−3068.

51. Cox, R. P., and Bendall, D. S. (1972) The effects on cytochrome b-559$_{HP}$ and P546 of treatments that inhibit oxygen evolution by chloroplasts, *Biochim. Biophys. Acta 283*, 124−135.
52. Horton, P., and Croze, E. (1977) The relationship between the activity of chloroplast photosystem II and the midpoint oxidation−reduction potential of cytochrome b-559, *Biochim. Biophys. Acta 462*, 86−101.
53. Rich, P. R., and Bendall, D. S. (1980) The redox potentials of the b-type cytochromes of higher plant chloroplasts, *Biochim. Biophys. Acta 591*, 153−161.
54. Ortega, J. M., Hervas, M., and Losada, M. (1990) Distinctive stability of the reduced and oxidized forms of high-potential cytochrome b-559 in photosystem II particles, *Plant Sci. 68*, 71−75.
55. Kaminskaya, O., Kern, J., Shuvalov, V. A., and Renger, G. (2005) Extinction coefficients of cytochromes b559 and c550 of *Thermosynechococcus elongatus* and Cyt b559/PS II stoichiometry of higher plants, *Biochim. Biophys. Acta 1708*, 333−341.
56. Cramer, W. A., Fan, H. N., and Böhme, H. (1971) High and low potential states of the chloroplast cytochrome b-559 and thermodynamic control of non-cyclic electron transport, *Bioenergetics 2*, 289−303.
57. Renger, G. (1971) II. The acceleration of the deactivation reactions in the watersplitting system by certain chemicals, *Z. Naturforsch., B: Chem. Sci. 26*, 149−153.
58. Renger, G. (1972) The action of 2-anilinothiophenes as accelerators of the deactivation reactions in the watersplitting enzyme system of photosynthesis, *Biochim. Biophys. Acta 256*, 428−439.
59. Renger, G., Bouges-Bocquet, B., and Büchel, K.-H. (1973) The modification of the trapping properties within the photosynthetic watersplitting enzyme system Y, *Bioenergetics 4*, 491−505.
60. Hanssum, B., Dohnt, G., and Renger, G. (1985) On the mechanism of ADRY agent interaction with the photosystem II donor side, *Biochim. Biophys. Acta 806*, 210−220.
61. Homann, P. H. (1972) Actions of tetraphenylboron on the electron flow in photosystem II of isolated chloroplasts, *Biochim. Biophys. Acta 256*, 336−344.
62. Erixon, K., and Renger, G. (1974) The action of tetraphenylboron as a system II electron donor and its effect on the decay of the electrical field across the thylakoid membrane, *Biochim. Biophys. Acta 333*, 95−106.
63. Hanssum, B., Renger, G., and Weiss, W. (1985) Studies on the reaction mechanism of tetraphenylboron at the photosystem II donor side in isolated spinach chloroplasts, *Biochim. Biophys. Acta 808*, 243−251.
64. Cramer, W. A., and Böhme, H. (1972) High-potential cytochrome b-559 as a secondary quencher of chloroplast fluorescence in the presence of 3-(3,4-dichlorophenyl)-1,1-dimethylurea, *Biochim. Biophys. Acta 256*, 358−369.
65. Heber, U., Kirk, M. R., and Boardman, N. K. (1979) Photoreactions of cytochrome b-559 and cyclic electron flow in photosystem II of intact chloroplasts, *Biochim. Biophys. Acta 546*, 292−306.
66. Maroc, J., and Garnier, J. (1979) Photooxidation of the cytochrome b-559 in the presence of various substituted 2-anilinothiophenes and of some other compounds, in *Chlamydomonas reinhardtii*, *Biochim. Biophys. Acta 548*, 374−385.
67. Velthuys, B. R. (1981) Carotenoid and cytochrome b 559 reactions in photosystem II in the presence of tetraphenylboron, *FEBS Lett. 126*, 272−276.
68. Packham, N. K., and Barber, J. (1984) The light-intensity-dependence of the efficacy of 2-(3-chloro-4-trifluoromethyl)-anilino-3,5-dinitrothiophene (Ant2p) to inhibit the photosystem 2 reactions of chloroplasts, *Biochem. J. 221*, 513−520.
69. Barabas, K., and Garab, G. (1989) Two populations of the high-potential form of cytochrome b-559 in chloroplasts treated with 2-(3-chloro-4-trifluoromethyl)anilino-3,5-dinitrothiophene (Ant 2p), *FEBS Lett. 248*, 62−66.
70. Barabas, K., Kravcova, T., and Garab, G. (1993) Flash-induced reduction of cytochrome b-559 by Q_B^- in chloroplasts in the presence of protonofores, *Photosynth. Res. 36*, 59−64.
71. Rutherford, A. W., Zimmermann, J. L., and Mathis, P. (1984) The effect of herbicides on components of the PS II reaction centre measured by EPR, *FEBS Lett. 165*, 156−162.
72. Berthold, D. A., Babcock, G. T., and Yocum, C. F. (1981) A highly resolved, oxygen-evolving photosystem II preparation from spinach thlakoid membranes. EPR and electron-transport properties, *FEBS Lett. 134*, 231−234.
73. Völker, M., Ono, T., Inoue, Y., and Renger, G. (1985) Effect of trypsin on PS-II particles. Correlation between Hill-activity, Mn-abundance and peptide pattern, *Biochim. Biophys. Acta 806*, 25−34.
74. Porra, R. J., Thompson, W. A., and Kriedemann, P. E. (1989) Determination of accurate extinction coefficients and simultaneous equations for assaying chlorophylls a and b extracted with four different solvents: Verification of the concentration of chlorophyll standards by athomic absorption spectroscopy, *Biochim. Biophys. Acta 975*, 384−394.
75. Tischer, W., and Strotmann, H. (1977) Relationship between inhibitor binding by chloroplasts and inhibition of photosynthetic electron transport, *Biochim. Biophys. Acta 460*, 113−125.
76. Pfister, K., Radosevich, S. R., and Arntzen, C. J. (1979) Modification of herbicide binding to photosystem II in two biotypes of *Senecio vulgaris* L., *Plant Physiol. 64*, 995−999.
77. Laasch, H., Pfister, K., and Urbach, W. (1981) Comparative binding of photosystem II-herbicides to isolated thylakoid membranes and intact green algae, Z. *Natutforsch., C: J. Biosci. 36*, 1041−1049.
78. Lavergne, J. (1982) Mode of action of 3-(3,4-dichlorophenyl)-1,1-dimethylurea. Evidence that the inhibitor competes with plastoquinone for binding to a common site on the acceptor side of photosystem II, *Biochim. Biophys. Acta 682*, 345−353.
79. Vermaas, W. F. J., Dohnt, G., and Renger, G. (1984) Binding and release kinetics of inhibitors of Q_A^- oxidation in thylakoid membranes, *Biochim. Biophys. Acta 765*, 74−83.
80. Oettmeier, W., and Masson, K. (1980) Synthesis and thylakoid membrane binding of the radioactively labeled herbicide dinoseb, *Pestic. Biochem. Physiol. 14*, 86−97.
81. Johanningmeier, U., Neumann, E., and Oettmeier, W. (1983) Interaction of a phenolic inhibitor with photosystem II particles, *J. Bioenerg. Biomembr. 15*, 43−66.
82. Kunz, W. S., and Konstantinov, A. A. (1983) Effect of b-c_1-site inhibitors on the midpoint potentials of mitochondrial cytochromes b, *FEBS Lett. 155*, 237−240.
83. Rich, P. R., Jeal, A. E., Madgwick, S. A., and Moody, A. J. (1990) Inhibitor effects on redox-linked protonations of the b haems of the mitochondrial bc_1 complex, *Biochim. Biophys. Acta 1018*, 29−40.
84. Howell, N., and Robertson, D. E. (1993) Electrochemical and spectral analysis of the long-range interactions between the Q_o and Q_i sites and the heme prosthetic groups in ubiquinol-cytochrome *c* oxidoreductase, *Biochemistry 32*, 11162−11172.
85. Smirnova, I. A., Hägerhäll, C., Konstantinov, A. A., and Hederstedt, L. (1995) HOQNO interaction with cytochrome b in succinate:menaquinone oxidoreductase from *Bacillus subtilis*, *FEBS Lett. 359*, 23−26.
86. Rothery, R. A., Blasco, F., Magalon, A., Asso, M., and Weiner, J. H. (1999) The hemes of *Escherichia coli* nitrate reductase A (NarGHI): Potentiometric effects of inhibitor binding to *Nar*I, *Biochemistry 38*, 12747−12757.
87. Clark, W. M. (1972) *Oxidation−Reduction Potentials of Organic Systems*, Waverley Press: Baltimore, MD.
88. Dutton, P. L., and Wilson, D. F. (1974) Redox potentiometry in mitochondrial and photosynthetic bioenergetics, *Biochim. Biophys. Acta 346*, 165−212.
89. Putrenko, I. I., Vasil'ev, S., and Bruce, D. (1999) Modulation of flash-induced photosystem II fluorescence by events occurring at the water oxidizing complex, *Biochemistry 38*, 10632−10641.
90. de Wijn, R., and van Gorkom, H. J. (2001) Kinetics of electron transfer from Q_A to Q_B in photosystem II, *Biochemistry 40*, 11912−11922.
91. Oettmeier, W., Masson, K., and Johanningmeier, U. (1982) Evidence for two different herbicide-binding proteins at the reducing side of photosystem II, *Biochim. Biophys. Acta 679*, 376−383.
92. Oettmeier, W., Masson, K., and Hecht, H-J. (2001) Heterocyclic ortho-quinones, a novel type of photosystem II inhibitors, *Biochim. Biophys. Acta 1504*, 346−351.
93. Oettmeier, W., and Renger, G. (1980) The function of diphenylamines as modifiers of photosystem II electron transport in isolated spinach chloroplasts, *Biochim. Biophys. Acta 593*, 113−124.
94. Ikeda, Y., Ohki, S., Koizumi, K., Tanaka, A., Watanabe, H., Kohno, H., van Rensen, J. J. S., Böger, P., and Wakabayashi, K.

(2003) Binding site of the novel 2-benzylamino-4-methyl-6-trifluoromethyl-1,3,5-triazine herbicides in the D1 protein of photosystem II, *Photosynth. Res. 77*, 35−43.
95. Vermaas, W. F. J., Arntzen, C. J., Gu, L.-Q., and Yu, C.-A. (1983) Interaction of herbicides and azidoquinones at a photosystem II binding site in the thylakoid membrane, *Biochim. Biophys. Acta 723*, 266−275.
96. Vermaas, W. F. J., Renger, G., and Arntzen, C. J. (1984) Herbicide/quinone binding interactions in photosystem II, *Z. Naturforsch., C: J. Biosci. 39*, 368−373.
97. Oettmeier, W., Masson. K., and Donner, A. (1988) Anthraquinone inhibitors of photosystem II electron transport, *FEBS Lett. 232*, 259−262.
98. Ohad, N., and Hirschberg, J. (1992) Mutations in the D1 subunit of photosystem II distinguish between quinone and herbicide binding sites, *Plant Cell 4*, 273−282.
99. Boschetti, A., Tellenbach, M., and Gerber, A. (1985) Covalent binding of 3-azido-monuron to thylakoids of DCMU-sensitive and -resistant strains of *Chlamydomonas reinhardtii*, *Biochim. Biophys. Acta 810*, 12−19.
100. Vermaas, W. F. J., and Atntzen, C. J. (1983) Synthetic quinones influencing herbicide binding and photosystem II electron transport. The effect of triazine-resistence on qiunone binding properties in thylakoid membranes, *Biochim. Biophys. Acta 725*, 483−491.
101. Oettmeier, W., Masson, K., Fedtke, C., Konze, J., and Schmidt, R. R. (1982) Effect of different photosystem II inhibitors on chloroplasts isolated from species either susceptible or resistant toward s-triazine herbicides, *Pestic. Biochem. Physiol. 18*, 357−367.
102. Oettmeier, W., and Masson, K. (1982) Picrate as an inhibitor of photosystem II in photosynthetic electron transport, *Eur. J. Biochem. 122*, 163−167.
103. Mattoo, A. K., Hoffman-Falk, H., Marder, J. B., and Edelman, M. (1984) Regulation of protein metabolism: Coupling of photosynthetic electron transport to in vivo degradation of the rapidly metabolized 32-kilodalton protein of the chloroplast membranes, *Proc. Natl. Acad. Sci. U.S.A. 81*, 1380−1384.
104. Kyle, D. J., Ohad, I., and Arntzen, C. J. (1984) Membrane protein damage and repair: Selective loss of a quinone−protein function in chloroplast membranes, *Proc. Natl. Acad. Sci. U.S.A. 81*, 4070−4074.
105. Kuhn, M., and Böger, P. (1990) Studies on the light-induced loss of the D1 protein in photosystem-II membrane fragments, *Photosynth. Res. 23*, 291−296.
106. Trebst, A. (1991) A contact site between the two reaction center polypeptides of photosystem II is involved in photoinhibition, *Z. Naturforsch., C: J. Biosci. 46*, 557−562.
107. Gong, H., and Ohad, I. (1991) The PQ/PQH_2 ratio and occupancy of photosystem II-Q_B site by plastoquinone control the degradation of D1 protein during photoinhibition in vivo, *J. Biol. Chem. 266*, 21293−21299.
108. Jansen, M. A. K., Depka, B., Trebst, A., and Edelman, M. (1993) Engagement of specific sites in the plastoquinone niche regulates degradation of the D1 protein in photosystem II, *J. Biol. Chem. 268*, 21246−21252.
109. Zer, H., and Ohad, I. (1995) Photoinactivation of photosystem II induces changes in the photochemical reaction center II abolishing the regulatory role of the Q_B site in the D1 protein degradation, *Eur. J. Biochem. 231*, 448−453.
110. Krieger-Liszkay, A., and Rutherford, A. W. (1998) Influence of herbicide binding of the redox potential of the quinone acceptor in photosystem II: Relevance to photodamage and phytotoxicity, *Biochemistry 37*, 17339−17344.
111. Rutherford, A. W., and Krieger-Liszkay, A. (2001) Herbicide-induced oxidative stress in photosystem II, *Trends Biochem. Soc. 26*, 648−653.
112. Renger, G. (1976) Studies on the structural and functional organization of system II of photosynthesis. The use of trypsin as a structurally selective inhibitor at the outer surface of the thylakoid membrane, *Biochim. Biophys. Acta 440*, 287−300.
113. Regitz, G., and Ohad, I. (1976) Trypsin-sensitive photosynthetic activities in chloroplast membranes from *Chlamydomonas reinhardtii*, y-1, *J. Biol. Chem. 251*, 247−252.
114. Böger, P., and Kunert, K.-J. (1979) Differential effects of herbicides upon trypsin-treated chloroplasts, *Z. Naturforsch., C: J. Biosci. 34*, 1015−1020.
115. Tischer, W., and Strotmann, H. (1979) Some properties of the DCMU-binding site in chloroplasts, *Z. Naturforsch., C: J. Biosci. 34*, 992−995.
116. Trebst, A. (1979) Inhibition of photosynthetic electron flow by phenol and diphenylether herbicides in control and trypsin-treated chloroplasts, *Z. Naturforsch., C: J. Biosci. 34*, 986−991.
117. Mattoo, A. K., Pick, U., Hoffman-Falk, H., and Edelman, M. (1981) The rapidly metabolized 32,000-dalton polypeptide of the chloroplast is the "proteinaceous shield" regulating photosystem II electron transport and mediating diuron herbicide sensitivity, *Proc. Natl. Acad. Sci. U.S.A. 78*, 1572−1576.
118. Renger, G., Hagemann, R., and Vermaas, W. F. J. (1984) Studies on the functional mechanism of system II herbicides in isolated chloroplasts, *Z. Naturforsch., C: J. Biosci. 39*, 362−367.
119. Trebst, A., Depka, B., Kraft, B., and Johanningmeier, U. (1988) The Q_B site modulates the conformation of the photosystem II reaction center polypeptides, *Photosynth. Res. 18*, 163−177.
120. Renger, G., Fromme R., and Hagemann, R. (1988) The modification of atrazine binding by the redox state of the endogenous high-spin iron and by specific proteolytic enzymes in photosystem II membrane fragments and intact thylakoids, *Biochim. Biophys. Acta 935*, 173−183.
121. Mathis, P., and Rutherford, A. W. (1984) Effect of phenolic herbicides on the oxygen-evolving side of photosystem II. Formation of the carotenoid cation, *Biochim. Biophys. Acta 767*, 217−222.
122. Trebst, A. (1986) The topology of the plastoquinone and herbicide binding peptides of photosystem II in the thylakoid membrane, *Z. Naturforsch., C: J. Biosci. 41*, 240−245.
123. Roberts, A. G., Gregor, W., Britt, R. D., and Kramer, D. M. (2003) Acceptor and donor-side interactions of phenolic inhibitors in photosystem II, *Biochim. Biophys. Acta 1604*, 23−32.
124. Schenck, C. C., Diner, B., Mathis, P., and Satoh, K. (1982) Flash-induced carotenoid radical cation formation in photosystem II, *Biochim. Biophys. Acta 680*, 216−227.
125. Packham, N. K., and Ford, R. C. (1986) Deactivation of the photosystem II oxidation (S) states by 2-(3-chloro-4-trifluoromethyl)anilino-3,5-dinitrothiophene (ANT2p) and the putative role of carotenoid, *Biochim. Biophys. Acta 852*, 183−190.
126. Hideg, E., and Demeter, S. (1986) Comparison of the decay of slow delayed luminescence in triazine-susceptible and -resistant biotypes of *Erigeron canadensis* L., *FEBS Lett. 200*, 139−143.
127. Chow, W. S, Hope, A. B., and Anderson, J. M. (1990) A reassessment of the use of herbicide binding to measure photosystem II reaction centres in plant thylakoids, *Photosynth. Res. 24*, 109−113.
128. Jursinic, P. A., McCarthy, S. A., Bricker, T. M., and Stemler, A. (1991) Characteristics of two atrazine-binding sites that specifically inhibit photosytem II function, *Biochim. Biophys. Acta 1059*, 312−322.
129. Oettmeier, W., Masson, K., and Johanningmeier, U. (1980) Photoaffinity labelling of the photosystem II herbicide binding protein, *FEBS Lett. 118*, 267−270.
130. Satoh, K., Katoh, S., Dostatni, R., and Oettmeier, W. (1986) Herbicide and plastoquinone-binding proteins of photosystem II reaction center complexes from the thermophilic cyanobacterium, *Synechococcus* sp., *Biochim. Biophys. Acta 851*, 202−208.
131. Etienne, A. L. (1974) New results on the properties of photosystem II centers blocked by 3-(3,4-dichlorophenyl)-1,1-dimethylurea in their different photoactive states, *Biochim. Biophys. Acta 333*, 320−330.
132. Pfister, K., and Schreiber, U. (1984) Comparison of diuron- and phenol-type inhibitors: Additional inhibitory action at the photosystem II donor site, *Z. Naturforsch., C: J. Biosci. 39*, 389−392.
133. Carpentier, R., Fuerst, E. P., Nakatani, H. Y., and Arntzen, C. J. (1985) A second site for herbicide action in photosystem II, *Biochim. Biophys. Acta 808*, 293−299.
134. Vasil'ev, I. R., Matorin, D. N., Lyadsky, V. V., and Venediktov, P. S. (1988) Multiple action sites for photosystem II herbicides as revealed by delayed fluorescence, *Photosynth. Res. 15*, 33−39.
135. Okayama, S., and Butler, W. L. (1972) Extraction and reconstitution of photosystem II, *Plant Physiol. 49*, 769−774.
136. Cox, R. P., and Bendall, D. S. (1974) The functions of plastoquinone and β-carotene in photosystem II of chloroplasts, *Biochim. Biophys. Acta 347*, 49−59.

137. Roncel, M., Boussac, A., Zurita, J. L., Bottin, H., Sugiura, M., Kirilovsky, D., and Ortega, J. M. (2003) Redox properties of the photosystem II cytochromes b559 and c550 in the cyanobacterium *Thermosynechococcus elongatus*, *J. Biol. Inorg. Chem. 8*, 206−216.
138. Barber, J., and De Las Rivas, J. (1993) A functional model for the role of cytochrome b_{559} in the protection against donor and acceptor side photoinhibition, *Proc. Natl. Acad. Sci. U.S.A. 90*, 10942−10946.
139. Nedbal, L., Samson, G., and Whitmarsh, J. (1992) Redox state of a one-electron component controls the rate of photoinhibition of photosystem II, *Proc. Natl. Acad. Sci. U.S.A. 89*, 7929−7933.
140. Gadjieva, R., Mamedov, F., Renger, G., and Styring, S. (1999) Interconversion of low- and high-potential forms of cytochrome b559 in tris-washed photosystem II membranes under aerobic and anaerobic conditions, *Biochemistry 38*, 10578−10584.

BI0613022